CHAPTER IV
RESULTS AND DISCUSSION

4.1 Benzoxazine Monomer Characterization

BZ synthesized by using phenol, ρ-formaldehyde, and tetraethylenepentamine (TEPA). The chemical structure of the benzoxazine are confirmed by FTIR spectroscopy, as shown in Figure 4.1. The presence of cyclic ether of benzoxazine structure is confirmed by the absorbance peak at 1,248 cm^{-1} assigned to the asymmetric stretching mode of the C-O-C group. The characteristic vibration of benzene with an attached oxazine ring is located at 933 cm^{-1}. The final structure of benzoxazine is also revealed by the peak at 1,486 cm^{-1}, which is significant for the vibration of the trisubstituted benzene ring. As expected, sharp peaks are observed at 1,344 cm^{-1} attributed to the C-N stretching vibration.

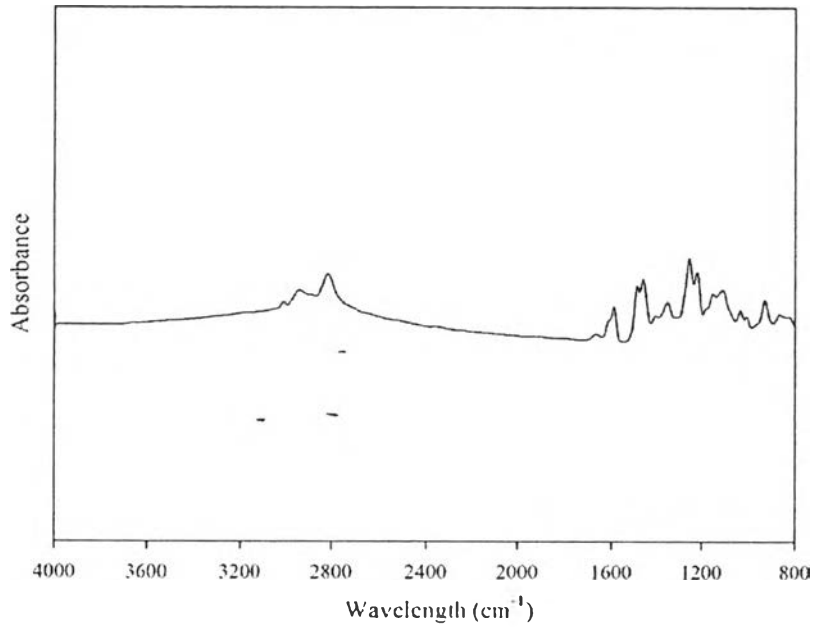

Figure 4.1 FTIR spectra of BZ.

In order to investigate the degree of curing, the uncured and cured samples are subjected to thermal analysis. The DSC thermograms of the uncured and cured BZ are given in Figures 4.2 and 4.3, respectively. As seen in Figure 4.2, an exothermic peak is observed due to the ring opening polymerization. The onset of the exotherm starts at 150.6 °C and reaches the maximum at 180.2 °C. On the other hand, no exothermic peak around 180 °C is seen in the cured BZ, as shown in Figure 4.3. It can be explained that the monomer polymerization is already finished prior to the DSC analysis. The DSC thermograms confirm that the BZ monomer can polymerize to PBZ at 180 °C.

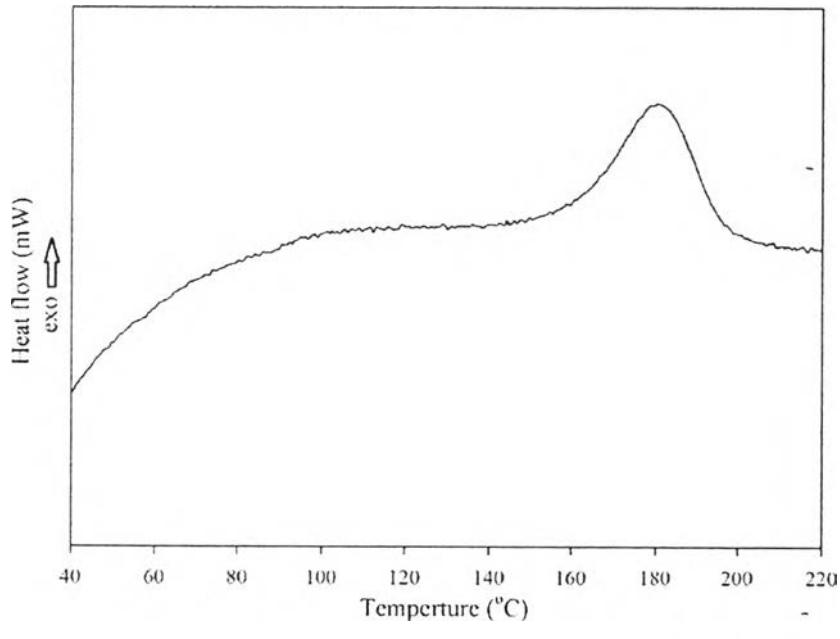

Figure 4.2 DSC thermogram of BZ.

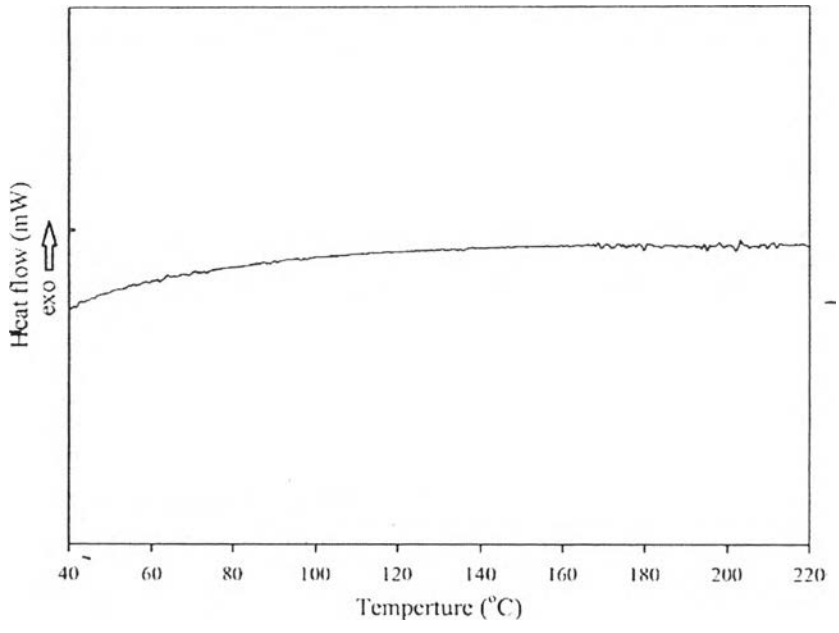

Figure 4.3 DSC thermogram of PBZ.

4.2 Adsorbent Characterization

BZ with different loadings were impregnated on the CSAC. The amounts of BZ impregnated on the CSAC were determined by UV-Vis spectroscopy. The concentrations of BZ solutions were measured using absorbance at 376 nm for methanol and at 279 nm for chloroform, which are used as a solvent for the impregnation. According to Beer-Lambert law, a calibration curve was constructed by absorbance at different BZ concentrations. The absorbance of the BZ solutions, which was filtered after impregnation, was measured and could be calculated to the final concentration. Table 4.1 shows the amounts of BZ impregnated on the CSAC, which were calculated by mass balance. Higher concentration of the BZ solution increases the amount of impregnated BZ due to the increased driving force (concentration gradient) of diffusion in the impregnation step.

Table 4.1 Amounts of BZ impregnated on the CSAC

Solvent	Initial concentration of BZ solution (g/L)	BZ impregnated on CSAC (wt% BZ)
Methanol	0.1	0.27
	0.5	0.92
	2.5	2.60
Chloroform	0.1	0.19
	0.5	0.58
	2.5	1.97

Interestingly, at the same initial concentration of BZ solution, using chloroform as a solvent results in the lower BZ impregnation on CSAC than using methanol.

The thermal stability of the adsorbents was investigated by thermogravimetric and differential thermal analysis (TG-DTA). The thermograms of the adsorbents are shown in Figures 4.4 – 4.5. Figure 4.4 shows the thermogram of the unmodified CSAC with one step weight loss due to the removal of volatile and moisture. Furthermore, the unmodified CSAC continues to be degraded or carbonized till 800 °C but cannot be detected as a step of weight loss due to the slight change in the weight loss and heat flow. From Figures 4.5, the thermograms show the weight loss in more than one step. The first step is below 100 °C for both impregnated CSACs with methanol and chloroform as a solvent, which is from the desorption of volatile and moisture. The second step of the impregnated CSAC using methanol as a solvent is around 200 °C, which is from the PBZ degradation. The second step of the impregnated CSAC using chloroform as a solvent is around 100 - 200 °C, which is from the desorption of chloroform that adsorbs on the surface of the CSAC (Abe *et al.*, 2001). The PBZ degradation of the impregnated CSAC using chloroform as a solvent is around 200 °C, and this is the third step of weight loss.

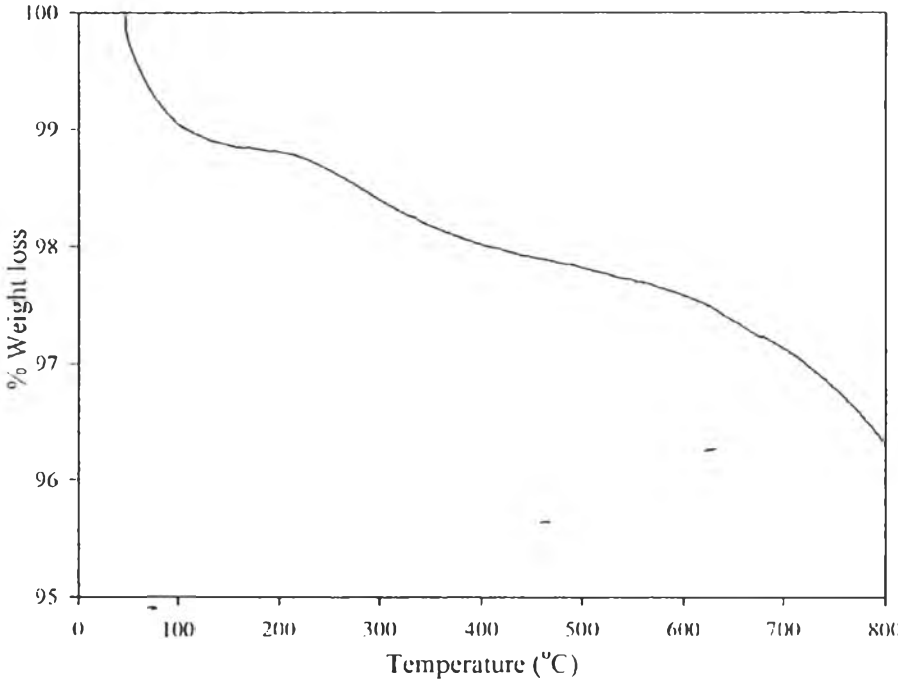

Figure 4.4 TGA thermogram of the unmodified CSAC.

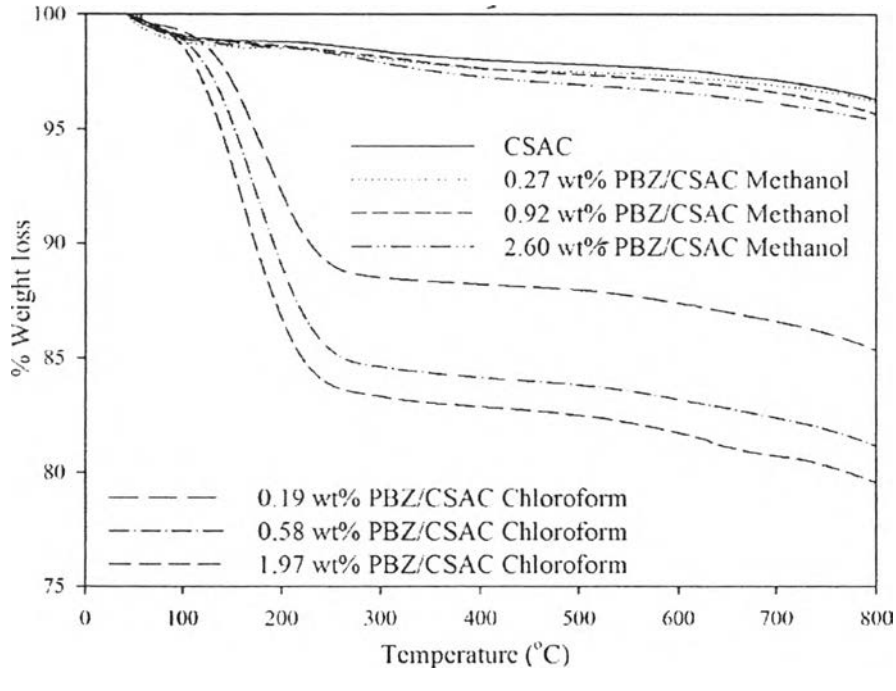

Figure 4.5 TGA thermograms of the unmodified CSAC and PBZ grafted CSAC.

From the thermal analysis results, the weight losses of both modified CSAC are higher with the increase in the amount of grafted PBZ. For the effect of solvent, at the same initial concentration of BZ solution, the impregnated CSAC using chloroform has higher weight loss than using methanol, as shown in Figure 4.5. The weight loss of impregnated CSAC using chloroform may be due to desorption of chloroform. Although the boiling point of chloroform is around 62 °C, chloroform can adsorb on the surface of the CSAC (Tsai *et al.*, 2008). There are some bondings between the surface and chloroform so it must use higher temperature around 100 - 200 °C for the desorption.

The functional groups in the adsorbents were detected by Fourier transform infrared spectroscopy (FTIR). The FTIR spectra of all adsorbents are shown in Figure 4.6. The wavelength at around 1,580 cm^{-1} shows the signal of N-H bond, which could represent the N-H functional group in the PBZ structure. In addition, the band of C-N stretching at around 1,100 cm^{-1} can be seen. The presence of the peak at 1,550 cm^{-1} represents the C=C bending of aromatics in the CSAC. The stretching vibrations from approximately 3,200 to 3,600 cm^{-1} are possibly due to the presence of surface hydroxylic groups and chemisorbed water (Swiatkowski *et al.*, 2004).

The elemental analysis of the unmodified CSAC and PSAC was investigated, as shown in Table 4.2. The results show that the amounts of each element of both ACs are similar. The main elements of both ACs are carbon and oxygen. Moreover, they have little hydrogen and nitrogen. The sulfur component can be detected in the unmodified CSAC, but not in the PSAC.

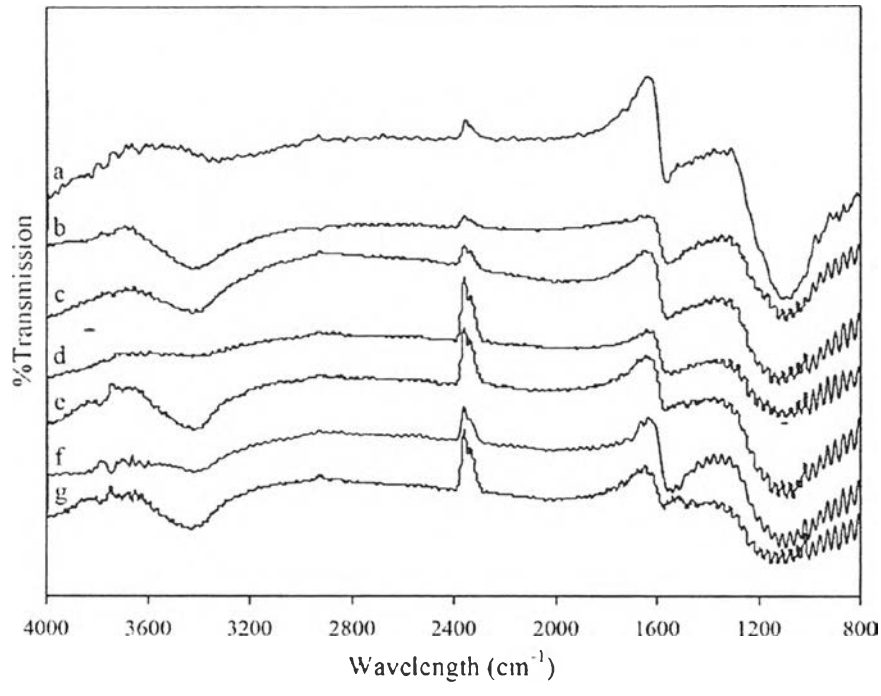

Figure 4.6 FTIR Spectra of the (a) CSAC, (b)-(d) 0.27, 0.92, and 2.60 wt% PBZ/CSAC using methanol, (e)-(g) 0.19, 0.58, and 1.97 wt% PBZ/CSAC using chloroform as a solvent.

Table 4.2 Elemental analysis of the AC

Adsorbent	%Carbon	%Hydrogen	%Nitrogen	%Oxygen	%Sulfur
CSAC	70.29	0.33	0.54	28.82	0.02
PSAC	74.15	0.16	0.46	25.23	-

The unmodified PSAC, CSAC and PBZ grafted CSAC were characterized for surface area and pore size analysis. Surface area, pore volume, and pore diameter of the adsorbents are shown in Table 4.3. The results show that the grafting of PBZ on the CSAC changes the surface properties and porosity. The surface area and pore volume decrease with the increase in the amount of PBZ with both solvents. Form the surface area result, the surface area of 0.27 wt% PBZ/CSAC using methanol as a solvent is 1,049 m^2/g, which is higher than 0.19 wt% PBZ/CSAC using Chloroform

as a solvent, 943 m^2/g, even the amount of PBZ on the surface area is higher. This results are consistent with the thermal analysis. That is chloroform can adsorb on the surface of CSAC and interrupt adsorption of BZ.

Table 4.3 Surface area, pore volume, and pore diameter of adsorbents

Adsorbent	Surface area (m^2/g)	Pore volume (cm^3/g)	Pore Diameter (Å)
PSAC	1,062	0.5336	9.26
CSAC	1,058	0.5277	10.07
0.27 wt% PBZ/CSAC Methanol	1,049	0.5169	6.66
0.92 wt% PBZ/CSAC Methanol	944	0.4717	6.14
2.60 wt% PBZ/CSAC Methanol	772	0.3821	6.14
0.19 wt% PBZ/CSAC Chloroform	943	0.4678	6.66
0.58 wt% PBZ/CSAC Chloroform	836	0.4152	6.14
1.97 wt% PBZ/CSAC Chloroform	772	0.3817	6.14

Nitrogen adsorption was a common technique to characterize porous materials. The adsorption isotherms could describe a type of material. Nitrogen isotherms of the adsorbents are shown in Figure 4.7 – 4.9. The result shows that 70% of pore volume is filled below $P/P^0 = 0.1$ in all adsorbents. This indicates that all the adsorbents are highly microporous materials. In addition, the adsorbents show the IUPAC type I or Langmuir isotherm.

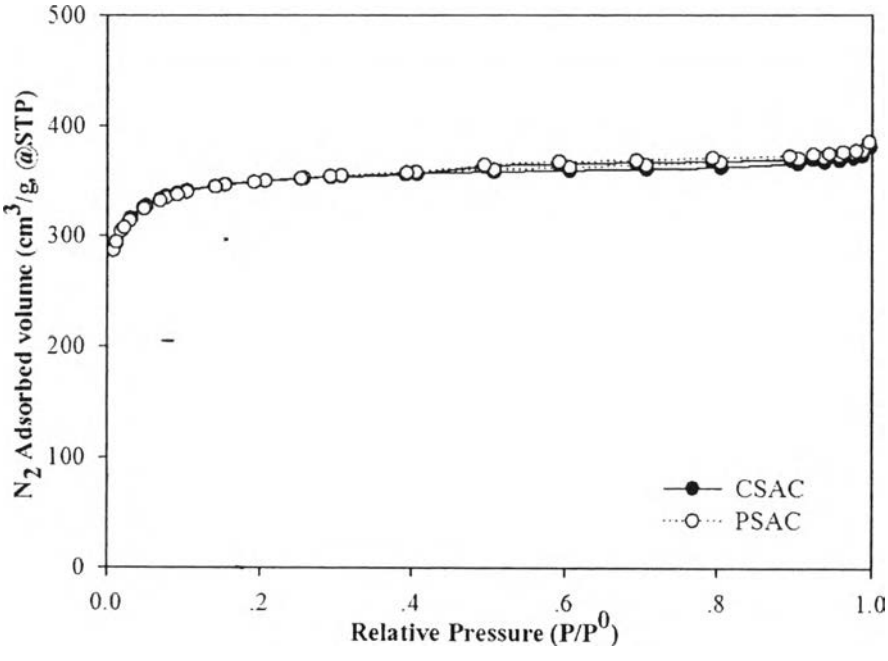

Figure 4.7 Nitrogen adsorption isotherms of unmodified CSAC and PSAC at -196 °C.

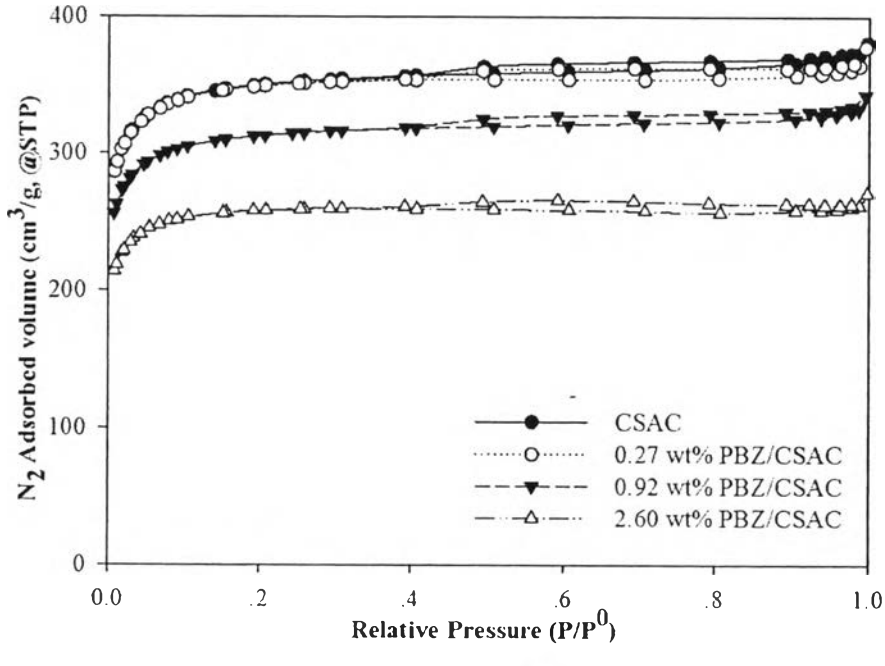

Figure 4.8 Nitrogen adsorption isotherms of unmodified CSAC and modified CSAC using methanol as solvent at -196 °C.

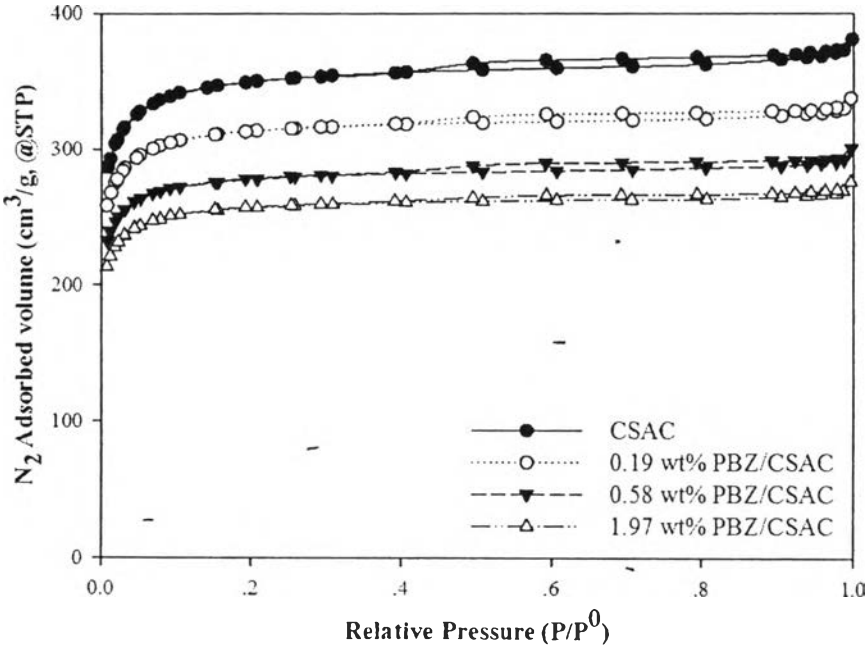

Figure 4.9 Nitrogen adsorption isotherms of unmodified CSAC and modified CSAC using chloroform as solvent at -196 °C.

The morphology of CSAC and PBZ grafted CSAC were assessed with the application of a scanning electron microscope. The SEM was operated at 15.0 kV of an accelerating voltage. Figure 4.10 shows the SEM morphologies of the unmodified CSAC and PBZ grafted CSAC using methanol as a solvent. The unmodified CSAC shows the original morphology of CSAC with a clear carbon surface (Figure 4.10a). When the PBZ is grafted onto the CSAC, the carbon surface is notably thickened by the PBZ coating; however, the sorbent still possesses considerable mesoporous porosity, allowing the transport of CO_2. Further increasing the PBZ loading, the pores are blocked and the carbon surface is fully covered by the PBZ, as shown in Figures 4.10b – 4.10d. The PBZ grafted CSAC using chloroform has the same pattern, as shown in Figure 4.11. These results are in agreement with the N_2 adsorption results.

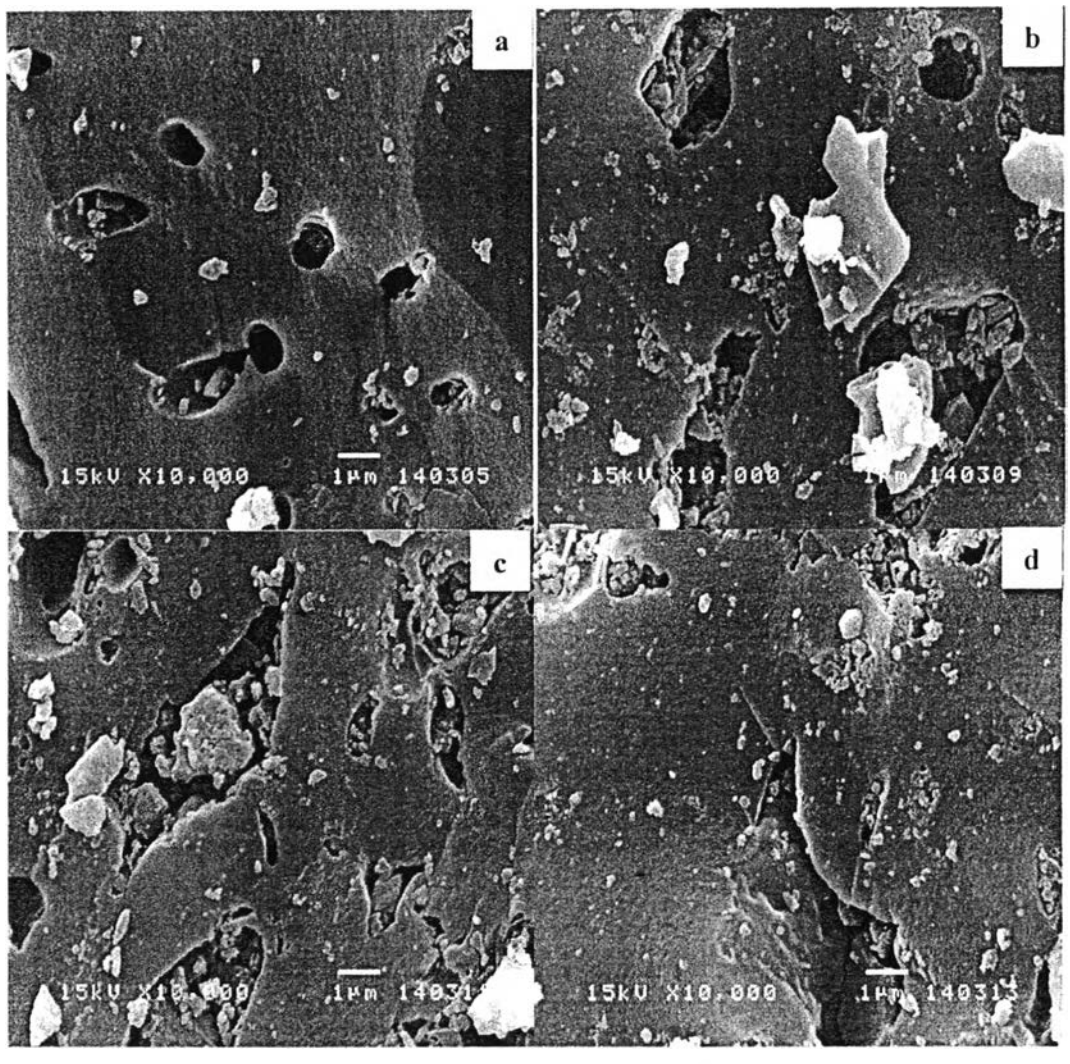

Figure 4.10 SEM micrographs of a) unmodified CSAC, b) 0.27 wt% PBZ/CSAC, c) 0.92 wt% PBZ/CSAC, and d) 2.60 wt% PBZ/CSAC using methanol as a solvent.

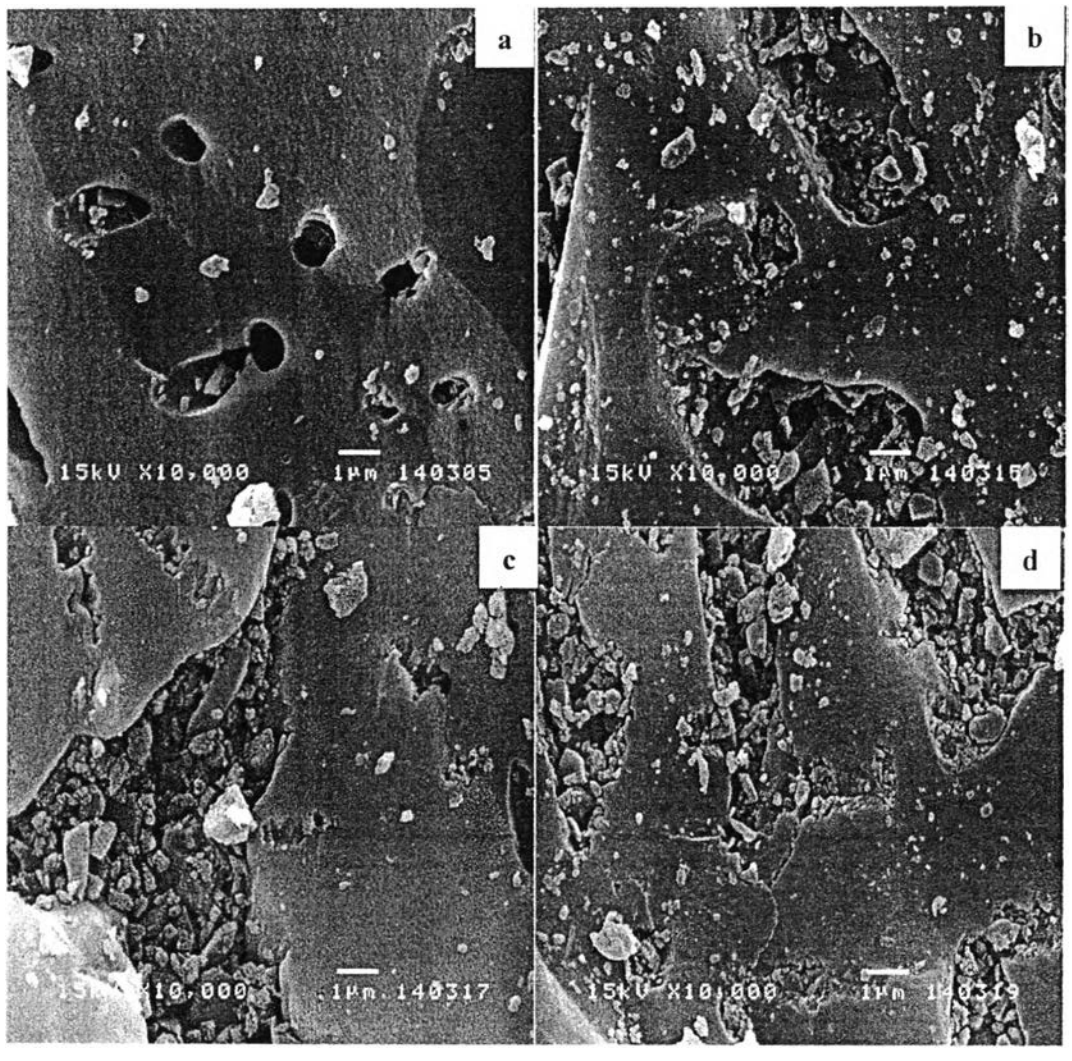

Figure 4.11 SEM micrographs of a) unmodified CSAC, b) 0.19 wt% PBZ/CSAC, c) 0.58 wt% PBZ/CSAC, and d) 1.97 wt% PBZ/CSAC using chloroform as a solvent.

4.3 CO_2 Adsorption on PSAC and CSAC

CO_2 adsorption isotherms of the unmodified CSAC and PSAC were constructed at 30, 50 and 75 °C, as shown in Figures 4.12 – 4.14, respectively. The results show that the unmodified CSAC has higher CO_2 adsorption capacity than the unmodified PSAC at every temperature. From Table 4.3, both ACs have about the same BET surface area (1,058 m^2/g for the unmodified CSAC and 1,062 m^2/g for the unmodified PSAC). One would expect about the same CO_2 adsorption capacity from

both ACs. The results, however, show otherwise. That may be due to the difference in the chemical composition of the samples. From Table 4.2, the unmodified CSAC has higher amount of oxygen than the unmodified PSAC. There are reports that the oxygen-containing groups enhance CO_2 sorption capacity. Gensterblum *et al.* (2014) promoted the hierarchical adsorption sites to describe the high energetic sites induced by the oxygen-containing groups. Liu and Wilcox (2012) observed oxygen-containing groups induced an efficient side-by-side CO_2 packing pattern by Grand Canonical Monte Carlo (GCMC) simulations.

Oxygen-containing functional groups seem to allow for enhanced electron transport and versatility depending on the acid–base nature of the adsorbent, with oxygen atoms acting as a Lewis base donating their electron density to the acidic carbon atoms of CO_2 molecules. Because of the higher electronegativities of the oxygen atoms than the carbon atom of CO_2 molecules, the carbon atom is more attracted to the embedded oxygen functional groups. The functionality-induced packing pattern makes it more efficient for CO_2 to occupy the limited pore space, with this change in packing configuration allowing for enhanced CO_2 adsorption capacity in the slit pores with hydroxyl and carbonyl functional groups than without (Liu and Wilcox, 2012).

From the results, the unmodified CSAC has higher CO_2 adsorption capacity than the PSAC. The CSAC is then used for further study.

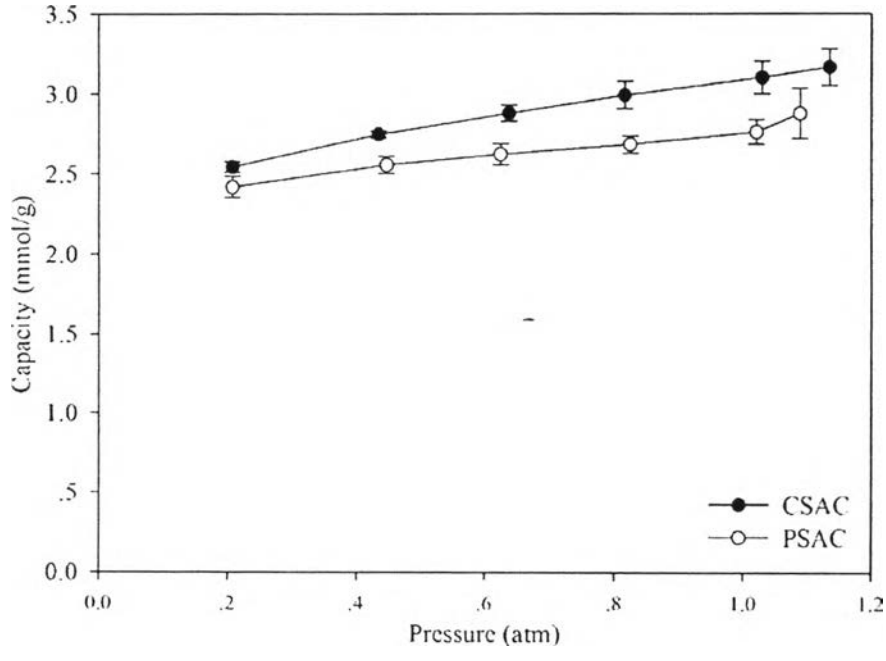

Figure 4.12 CO_2 adsorption isotherms of the unmodified CSAC and PSAC at 30 °C.

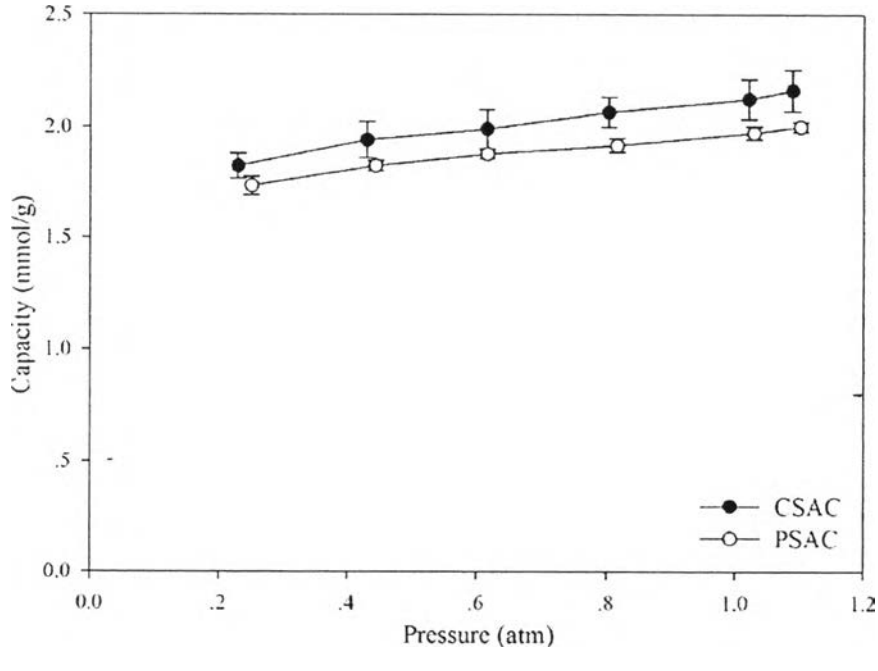

Figure 4.13 CO_2 adsorption isotherms of the unmodified CSAC and PSAC at 50 °C.

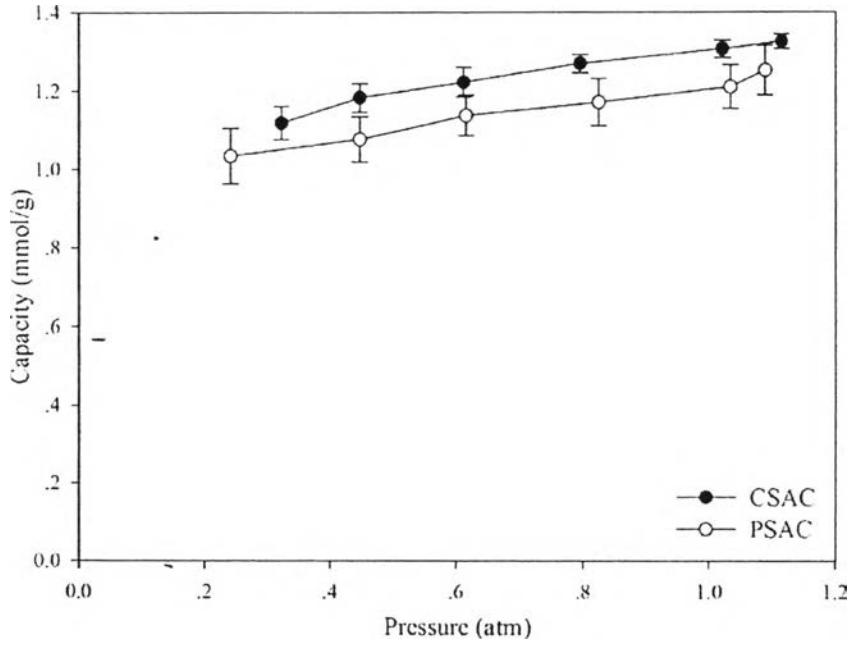

Figure 4.14 CO_2 adsorption isotherms of the unmodified CSAC and PSAC at 75 °C.

4.4 Effects of Solvents in the BZ Impregnation on CO_2 Adsorption

CO_2 adsorption isotherms of the impregnated CSAC using chloroform and methanol as a solvent were constructed at 30, 50, and 75 °C, as shown in Figures 4.15 – 4.16, 4.17 – 4.18, and 4.19 – 4.20, respectively. The solvents used for the BZ impregnation on the CSAC surface clearly affect the CO_2 adsorption capacity. The modified CSAC using chloroform as a solvent has lower CO_2 adsorption capacity than that using chloroform. Moreover, it has lower CO_2 capacity than the unmodified CSAC. There are reports that chloroform can be adsorbed by activated carbon. Urano *et al.* (1991) examined the capacity and rate of adsorption of various chlorinated organic compounds onto commercial granular activated carbons. Razvigorova *et al.* (1998) studied chloroform adsorption onto activated carbons made from apricot stones, lignites, and anthracite. Abe *et al.* (2001) investigated some raw materials of activated carbon, e.g., evergreen oak, bamboo, coconut shell, and Japanese cedar, for the removal of chloroform and other organic matters from drinking water. Shin *et al.* (2002) investigated the adsorption patterns of four kinds of aromatics and four kinds

of chlorinated compounds in raw land field gas by an activated carbon fixed bed. Tsai *et al.* (2008) investigated the adsorption characteristics of acetone, chloroform, and acetonitrile by sludge-derived adsorbent, commercial activated carbon, and two types of activated carbon fibers. From the literature, chloroform can easily adsorb on the CSAC surface. As the result, it decreases the surface area and blocks pore size of the CSAC. Form Table 4.3, the modified CSAC using chloroform has lower surface area than that using methanol even the amount of BZ on the surface is lower. Moreover, chloroform is expected to competitively adsorb on the CSAC surface with BZ. From Table 4.1, the amount of BZ on the CSAC surface using chloroform as a solvent is lower than that using methanol despite of the same initial concentration of BZ solution.

Consequently, methanol is then used as the solvent for the impregnation for further study.

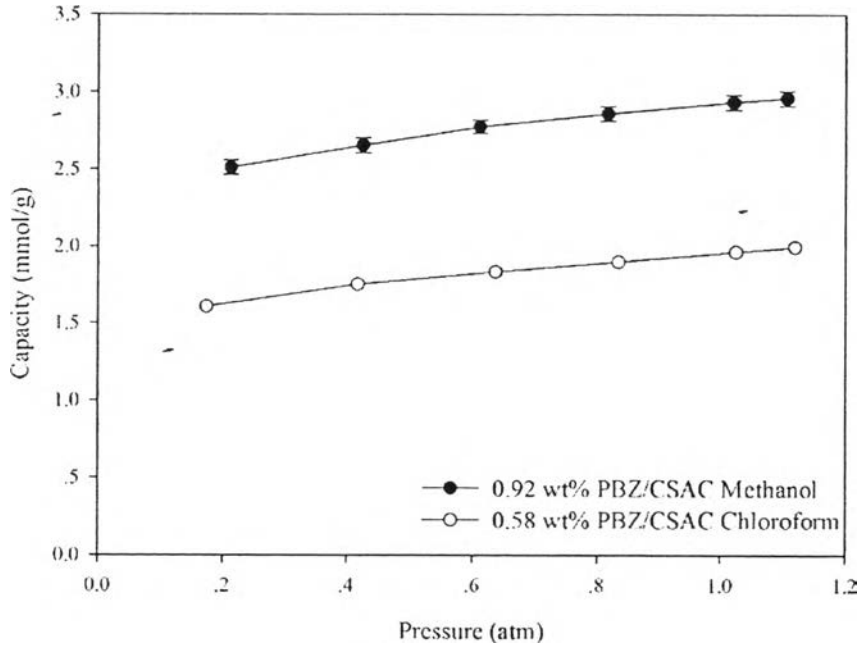

Figure 4.15 CO_2 adsorption isotherms of the PBZ/CSAC at 30 °C (initial concentration of BZ = 0.1 g/L).

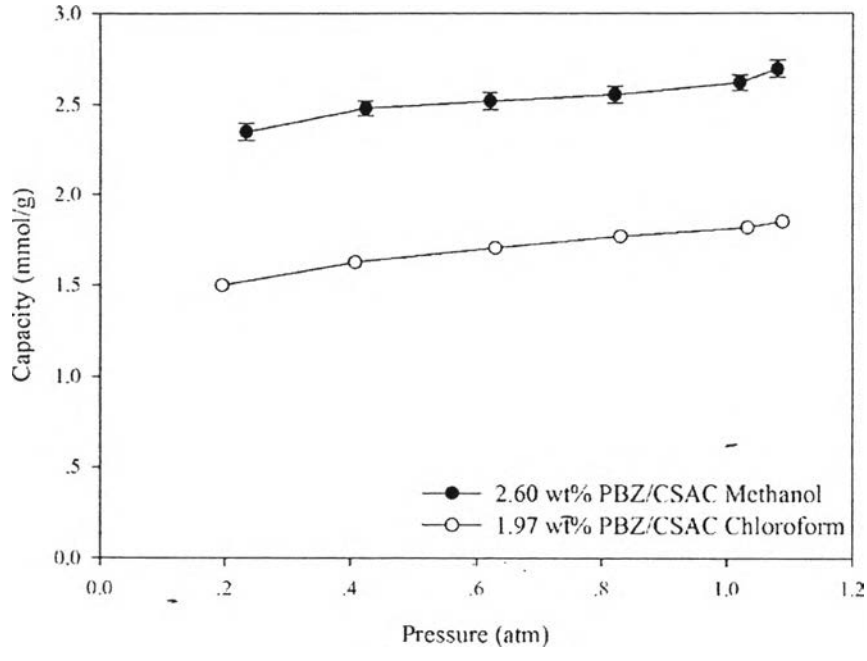

Figure 4.16 CO_2 adsorption isotherms of the PBZ/CSAC at 30 °C (initial concentration of BZ = 0.5 g/L).

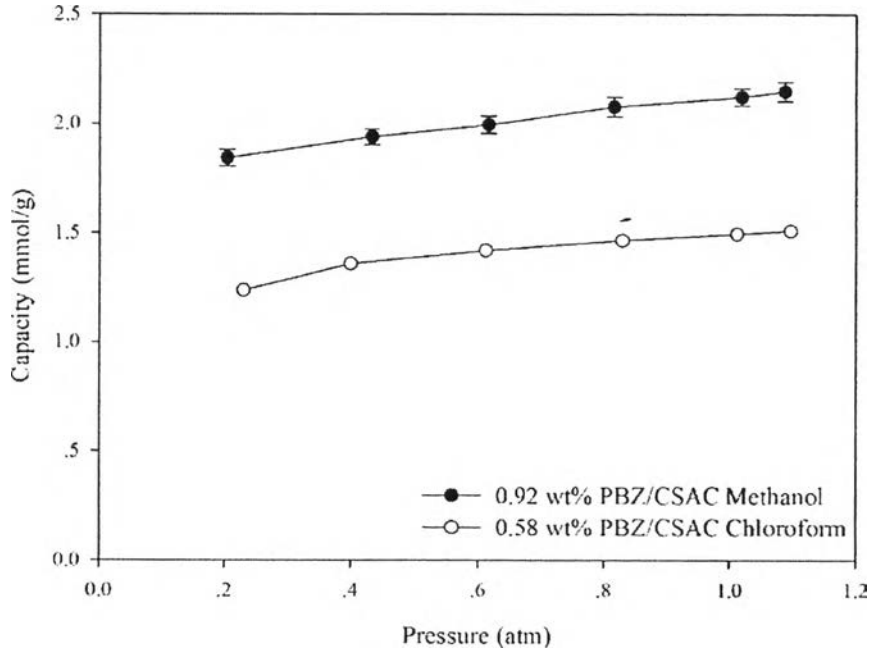

Figure 4.17 CO_2 adsorption isotherms of the PBZ/CSAC at 50 °C (initial concentration of BZ = 0.1 g/L).

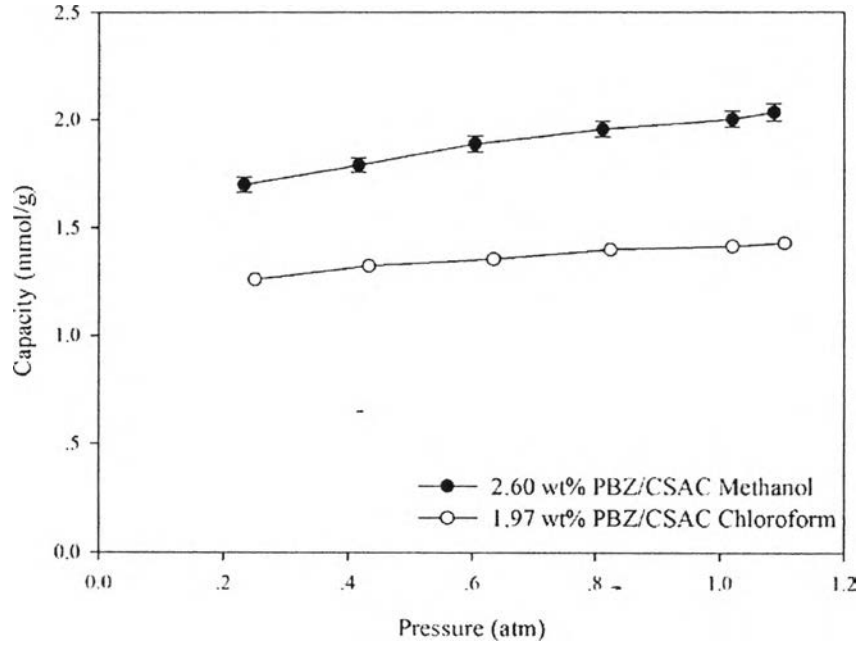

Figure 4.18 CO_2 adsorption isotherms of the PBZ/CSAC at 50 °C (initial concentration of BZ = 0.5 g/L).

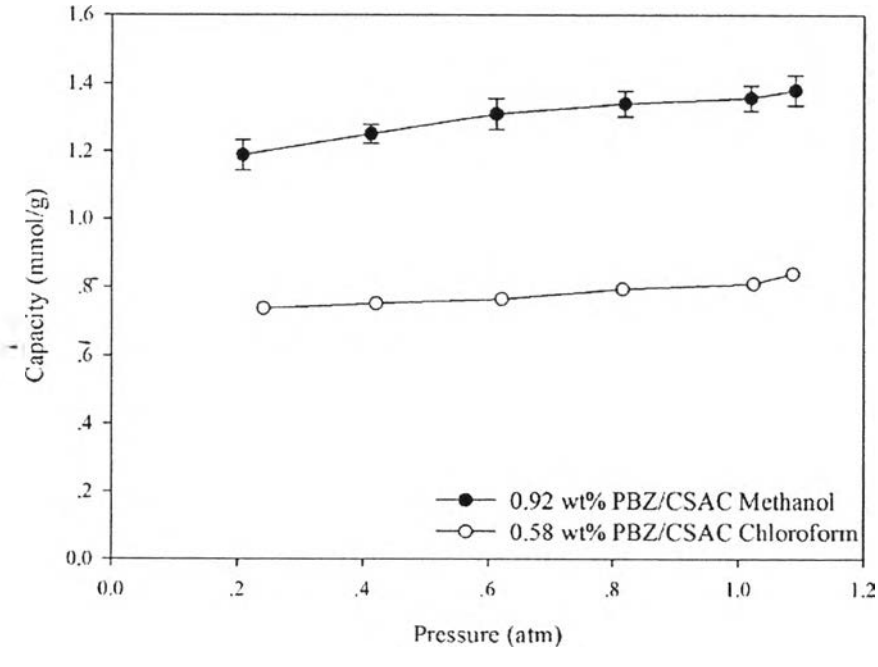

Figure 4.19 CO_2 adsorption isotherms of the PBZ/CSAC at 75 °C (initial concentration of BZ = 0.1 g/L).

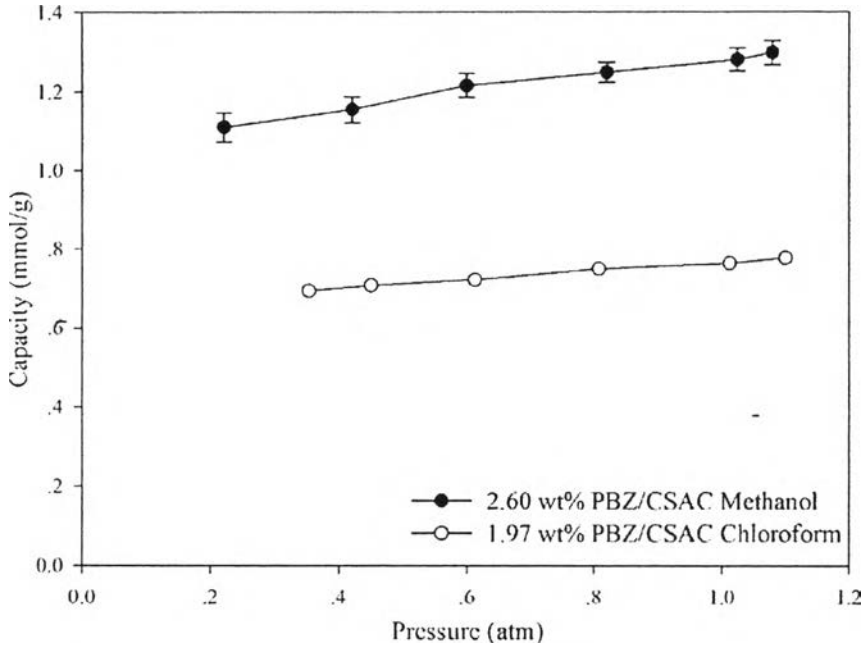

Figure 4.20 CO_2 adsorption isotherms of the PBZ/CSAC at 75 °C (initial concentration of BZ = 0.5 g/L).

4.5 Effects of PBZ Loading on CO_2 Adsorption

The influence of PBZ loading on the CO_2 adsorption of PBZ grafted CSAC was investigated at 30 - 75 °C, and the results are shown in Figures 4.21 - 4.23. Before PBZ is grafted, the CSAC alone shows CO_2 adsorption capacity of 3.02, 2.08, and 1.28 mmol/g at 30, 50, and 75 °C at 1 atm, respectively. At 30 °C, all modified CSACs have lower CO_2 adsorption capacity than the unmodified CSAC. It may be due to chemical reactions between the amine group and CO_2 are not preferred at the low temperature (Pipatsantipong, 2012). Also the adsorption at this temperature depends on the surface area as the adsorption is governed by the physisorption. From Table 4.3, the surface area of 0.27, 0.92, and 2.60 wt% PBZ/CSAC are 1,049, 944, and 772 m^2/g, respectively so the 0.27 wt% PBZ/CSAC has higher CO_2 adsorption capacity than 0.92 and 2.60 wt% PBZ/CSAC. Too high a loading of PBZ decreases the capacity because it decreases the surface area, hence, the extend of the physisorption.

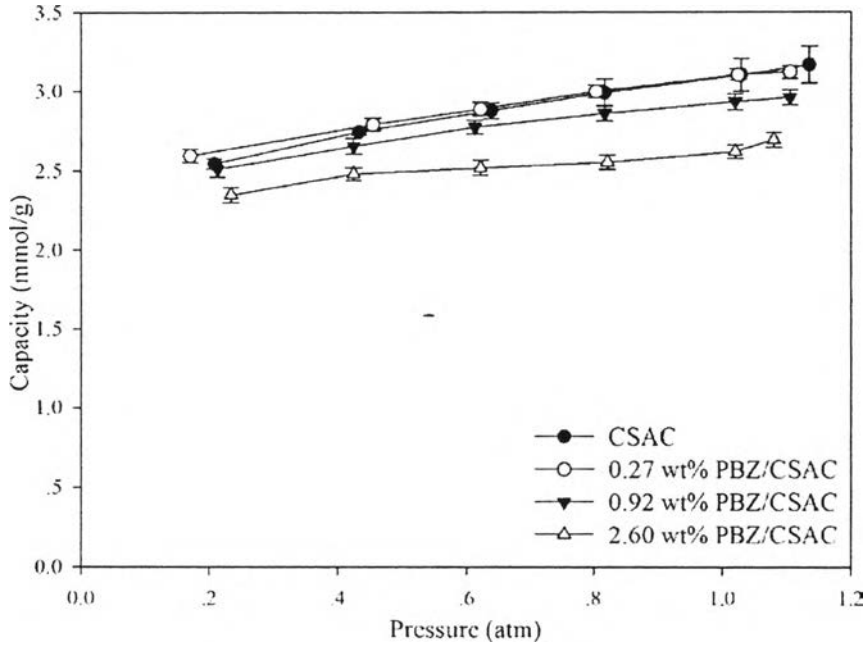

Figure 4.21 CO_2 adsorption isotherms of the unmodified CSAC and PBZ/CSAC at 30 °C.

At 50 °C (Figure 4.22), the CO_2 adsorption capacity of the modified CSAC ranges between 2.23, 2.07, and 1.97 mmol/g-adsorbent at 1 atm for 0.27, 0.92, and 2.60 wt% PBZ/CSAC, respectively. The 0.27 wt% PBZ/CSAC has significantly higher CO_2 adsorption capacity than the unmodified CSAC though the surface area and pore volume are lower. It implies that the chemical reaction is more favorable at this temperature. However, the adsorption capacity is lower than the unmodified CSAC when the amount of PBZ is increased to 0.92, and 2.60 wt%. Therefore, a balance between the chemisorption and physisorption is needed to increase the CO_2 adsorption capacity.

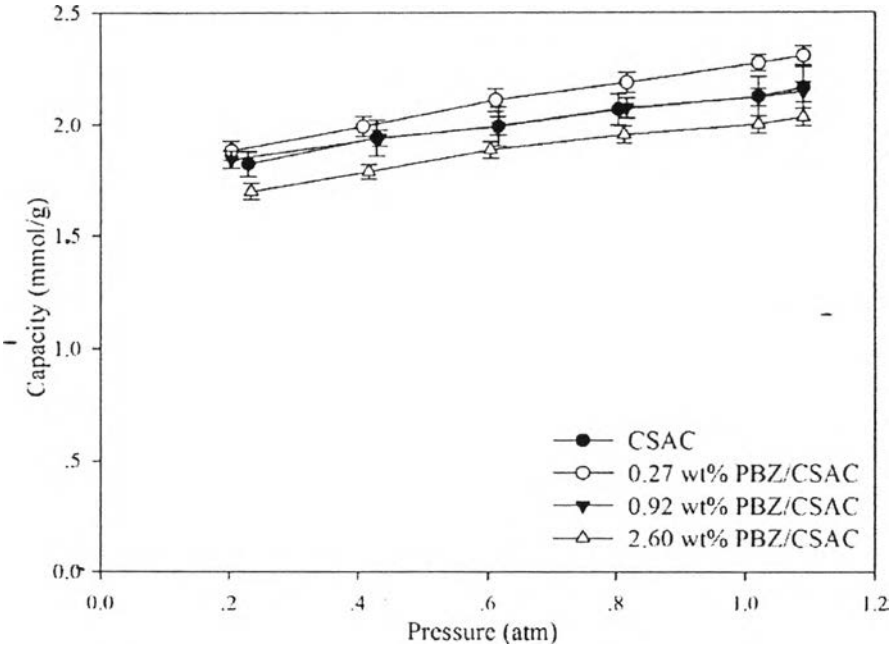

Figure 4.22 CO_2 adsorption isotherms of the unmodified CSAC and PBZ/CSAC at 50 °C.

At 75 °C (Figure 4.23), the CO_2 adsorption capacity is 1.42, 1.33, and 1.25 mmol/g-adsorbent at 1 atm for 0.27, 0.92, and 2.60 wt% PBZ/CSAC, respectively. Compared to the results at 50 °C, it is only the 0.27 wt% PBZ/CSAC that has higher CO_2 adsorption capacity than the unmodified CSAC. But at 75 °C, the 0.27 and 0.92 wt% PBZ/CSAC have higher CO_2 adsorption capacity than the unmodified CSAC. However, the adsorption capacity is lower than the unmodified CSAC when the amount of PBZ is increased to 2.60 wt%. This may be attributed to the pore filling effect that blocks the pores of the adsorbent preventing CO_2 to diffuse into the pores (Xu *et al.*, 2005a: Jadhav *et al.*, 2007). The results imply that an amount of PBZ on the CSAC should be high enough for the reaction with CO_2 but not too high to shield the physical properties of the CSAC.

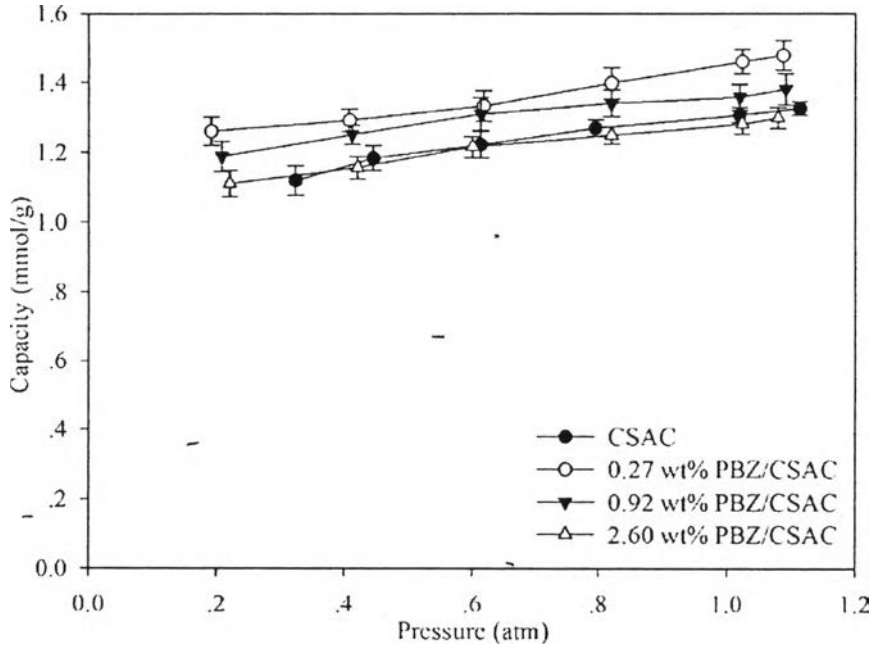

Figure 4.23 CO_2 adsorption isotherms of the unmodified CSAC and PBZ/CSAC at 75 °C.

4.6 Effects of Temperature on CO_2 Adsorption

CO_2 adsorption isotherms of the unmodified CSAC and PBZ grafted CSAC were constructed at 30, 50, and 75 °C, as shown in Figures 4.24 - 4.27. For the unmodified CSAC, the increase in the adsorption temperature reduces the CO_2 adsorption capacity because the physisorption of the CSAC is exothermic phenomenon or not favorable at the high adsorption temperature.

For the 0.27 wt% PBZ/CSAC (Figure 4.25), it can be observed that the CO_2 adsorption of modified CSAC has lower capacity than the unmodified CSAC at 30 °C. It may be due to chemical reactions between the amine group and CO_2 are not preferred at low temperature (Pipatsantipong, 2012). But it shows higher adsorption capacities than the unmodified CSAC at the 50 and 75 °C. The results confirm that the increase in the temperature facilitates the transfer of the adsorbed CO_2 molecules from the surface into the bulk of PBZ by overcoming the kinetic barrier (Ma *et al.*, 2009).

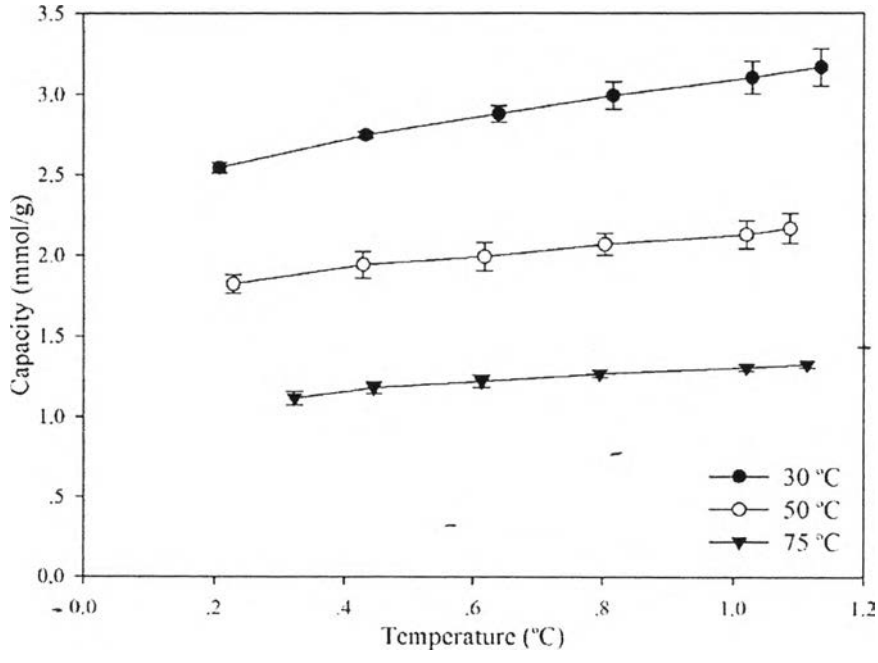

Figure 4.24 CO_2 adsorption isotherms of the unmodified CSAC at 30, 50, and 75 °C.

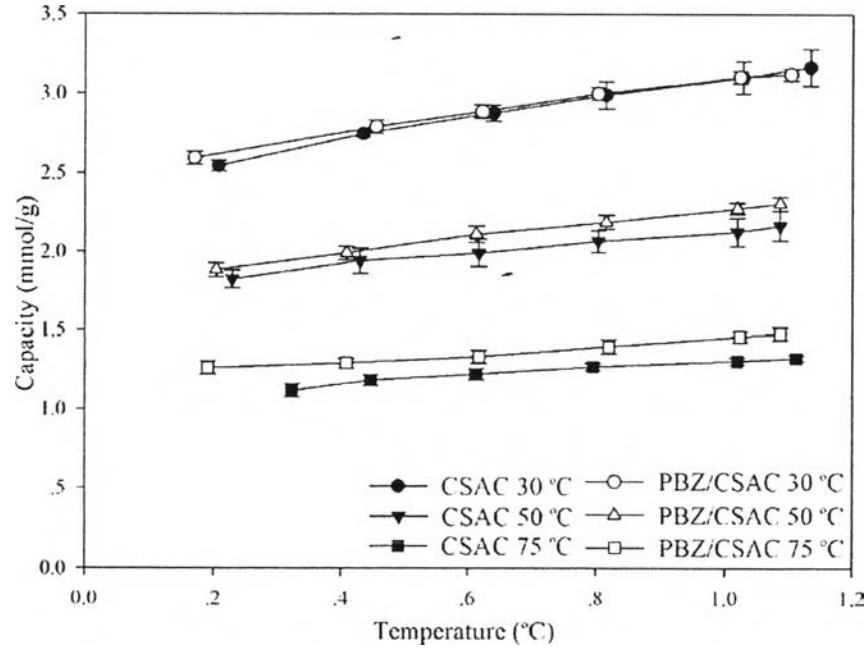

Figure 4.25 CO_2 adsorption isotherms of the unmodified CSAC and 0.27 wt% PBZ/CSAC at 30, 50, and 75 °C.

For the 0.92 wt% PBZ/CSAC (Figure 4.26), its adsorption capacity is lower than the unmodified CSAC at 30 and 50 °C. It may be due to the decrease in the surface area with the increase in the PBZ loading. So the optimum amount of PBZ loading is needed to increase the CO_2 adsorption capacity.

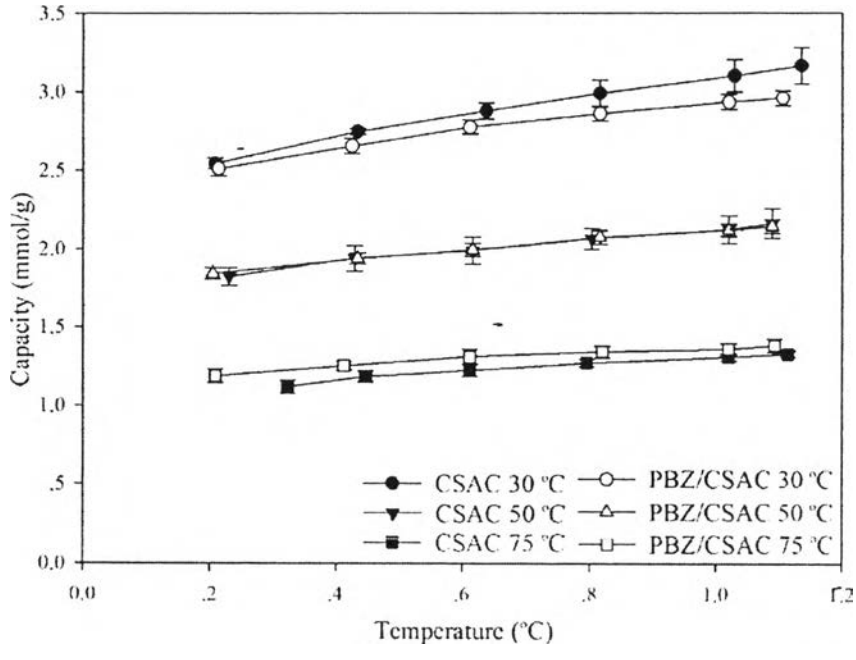

Figure 4.26 CO_2 adsorption isotherms of the unmodified CSAC and 0.92 wt% PBZ/CSAC at 30, 50, and 75 °C.

For the 2.60 wt% PBZ/CSAC (Figure 4.27), it can be observed that the unmodified CSAC has higher CO_2 adsorption capacity than the CSAC modified with PBZ at every temperature. PBZ cannot improve the CO_2 adsorption capacity even at the high temperature. The surface area and pore volume of 2.60 wt% PBZ/CSAC are decreased by the blockage of PBZ, as shown in Table 4.3. The results further confirm that a balance between the chemisorption and physisorption is essential.

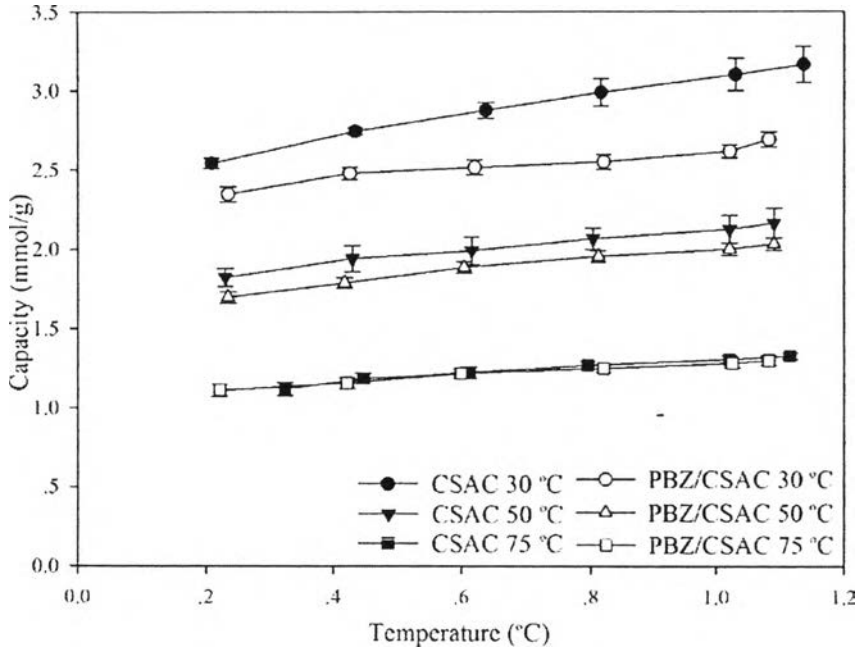

Figure 4.27 CO_2 adsorption isotherms of the unmodified CSAC and 2.60 wt% PBZ/CSAC at 30, 50, and 75 °C.

Table 4.4 CO_2 adsorption capacity of adsorbents at 30 °C and 1 atm

Adsorbent	CO_2 adsorption capacity (mmol/g adsorbent)
CSAC	3.02
0.27 wt% PBZ/CSAC	3.01
0.92 wt% PBZ/CSAC	2.88
2.60 wt% PBZ/CSAC	2.57

Table 4.5 CO_2 adsorption capacity of adsorbents at 50 °C and 1 atm

Adsorbent	CO_2 adsorption capacity (mmol/g adsorbent)
CSAC	2.08
0.27 wt% PBZ/CSAC	2.23
0.92 wt% PBZ/CSAC	2.08
2.60 wt% PBZ/CSAC	1.96

Table 4.6 CO_2 adsorption capacity of adsorbents at 75 °C and 1 atm

Adsorbent	CO_2 adsorption capacity (mmol/g adsorbent)
CSAC	1.28
0.27 wt% PBZ/CSAC	1.42
0.92 wt% PBZ/CSAC	1.32
2.60 wt% PBZ/CSAC	1.25

4.7 CO_2 Adsorption on Regenerated PBZ/CSAC

The adsorbent should not only have a high adsorption capacity and high selectivity, but also can be regenerated with relatively constant adsorption performance. After the adsorbent saturates with CO_2, the regeneration is needed to remove CO_2 from the adsorbent. The regeneration temperature of 120 °C was chosen to ensure that the volatile and adsorbed gas are completely desorbed, and the structures of the AC and PBZ are not destroyed (Ma *et al.*, 2009; Goeppert *et al.*, 2011). Figures 4.28 – 4.30 illustrate the adsorption capacity of the fresh and regenerated unmodified CSAC at 30, 50, and 75 °C, respectively. During the three cycles, the CO_2 adsorption capacity of the unmodified CSAC was not significantly changed, indicating that the desorption is complete and the desorption of CO_2 can be achieved at 120 °C. Table 4.7 shows the surface area of the fresh and regenerated

unmodified CSAC. The surface area of regenerated adsorbent is relatively constant compared to the fresh adsorbent.

Table 4.7 Surface area of fresh and regenerated CSAC

Adsorption Temperature °C	Adsorbent	Surface area (m^2/g)
30	CSAC	1,058
	1st regenerated CSAC	1,051
50	CSAC	1,058
	1st regenerated CSAC	1,042
75	CSAC	1,058
	1st regenerated CSAC	1,011

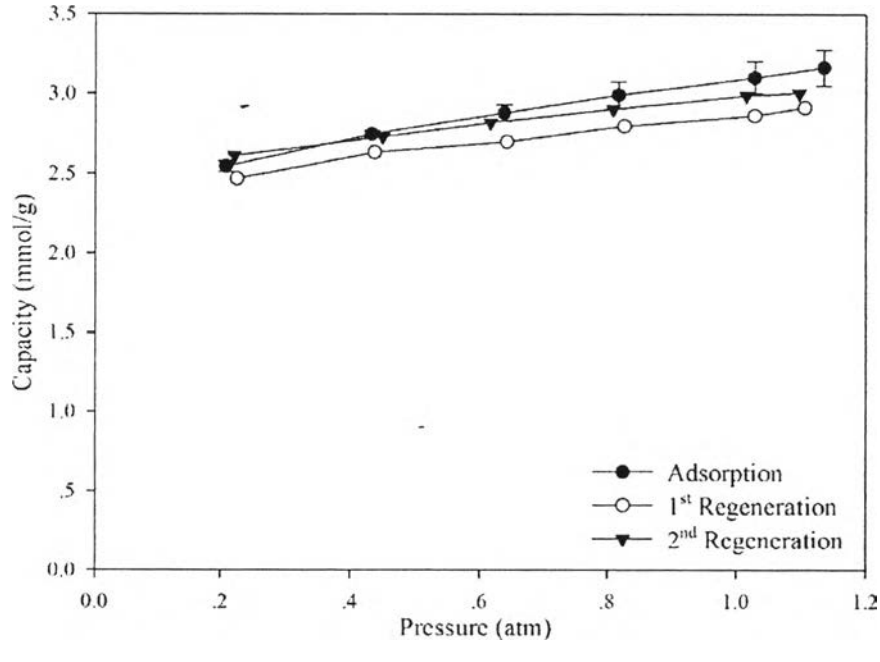

Figure 4.28 CO_2 adsorption isotherms at 30 °C of the CSAC and the regenerated CSAC.

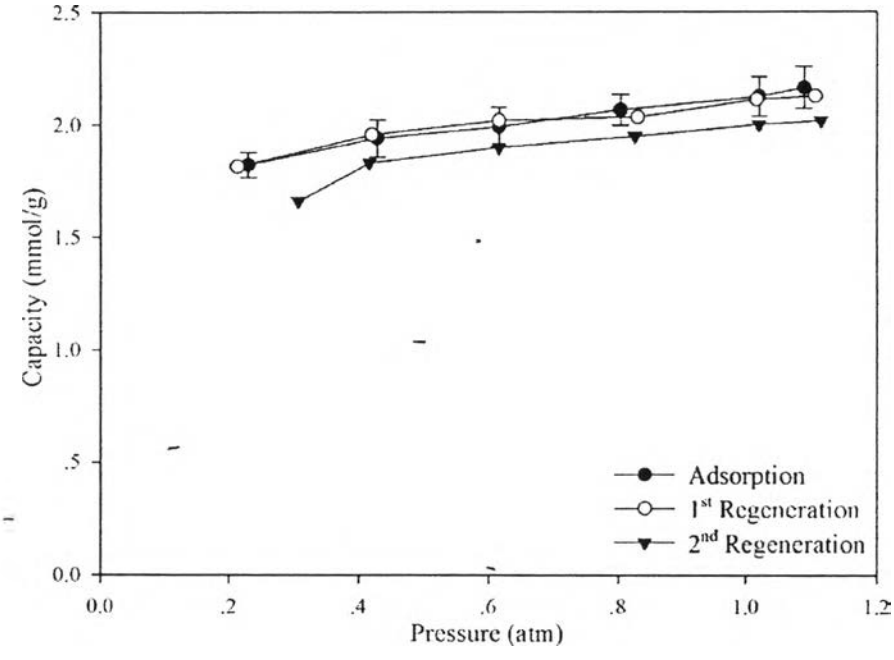

Figure 4.29 CO_2 adsorption isotherms at 50 °C of the CSAC and the regenerated CSAC.

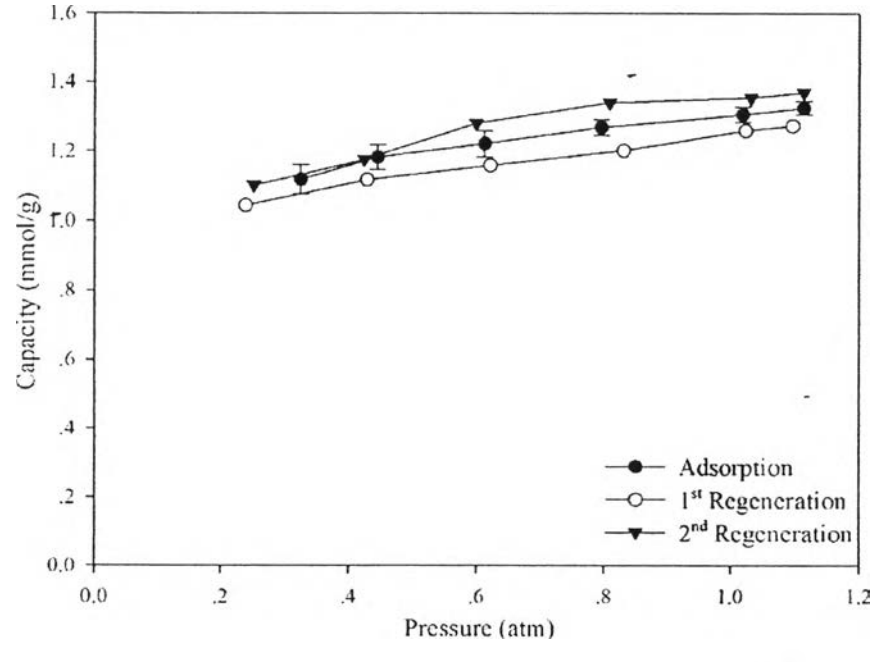

Figure 4.30 CO_2 adsorption isotherms at 75 °C of the CSAC and the regenerated CSAC.

The CO_2 adsorption on the regenerated of the modified CSAC is shown in Figures 4.31 – 4.39. The figures illustrate the adsorption capacity of the fresh and regenerated modified CSAC at 30, 50, and 75 °C, respectively. During the two cycles, the CO_2 adsorption capacity of the modified CSAC was not significantly changed. The results show that both adsorbents, the unmodified and modified CSAC, are the same efficiency to recovery. This implies that the PBZ grafted CSAC can be recovery completely at 120 °C.

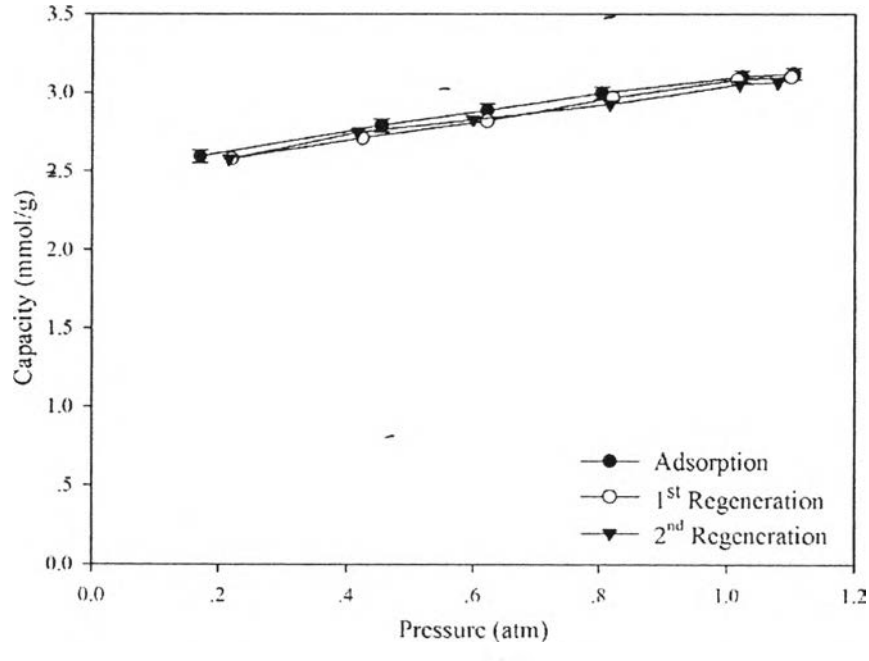

Figure 4.31 CO_2 adsorption isotherms at 30 °C of the 0.27 wt% PBZ/CSAC and the regenerated adsorbent.

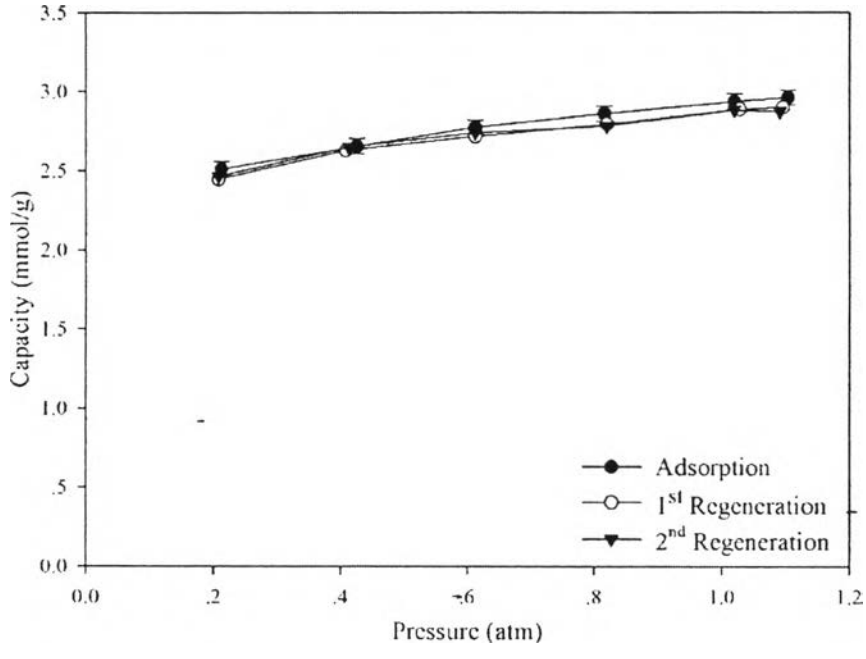

Figure 4.32 CO_2 adsorption isotherms at 30 °C of the 0.92 wt% PBZ/CSAC and the regenerated adsorbent.

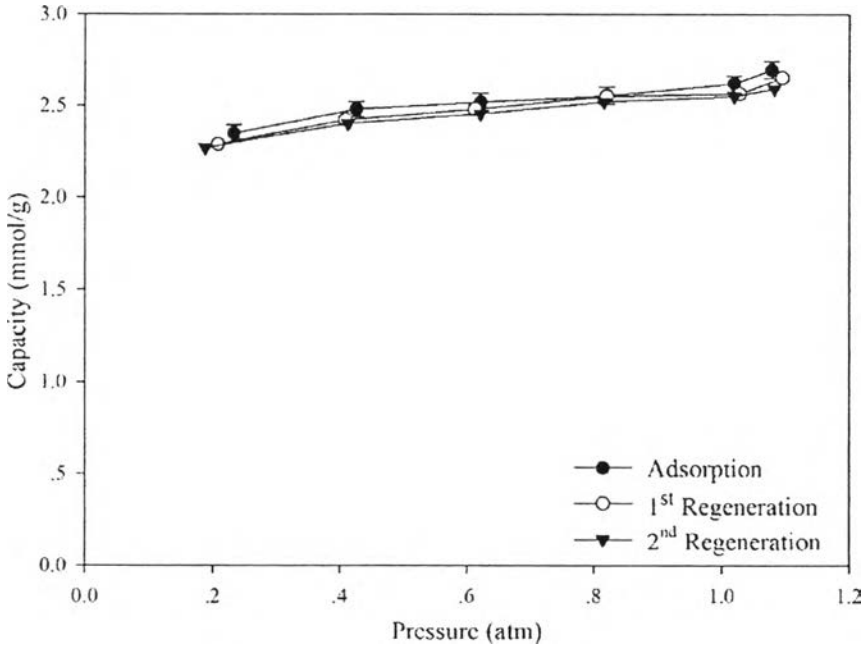

Figure 4.33 CO_2 adsorption isotherms at 30 °C of the 2.60 wt% PBZ/CSAC and the regenerated adsorbent.

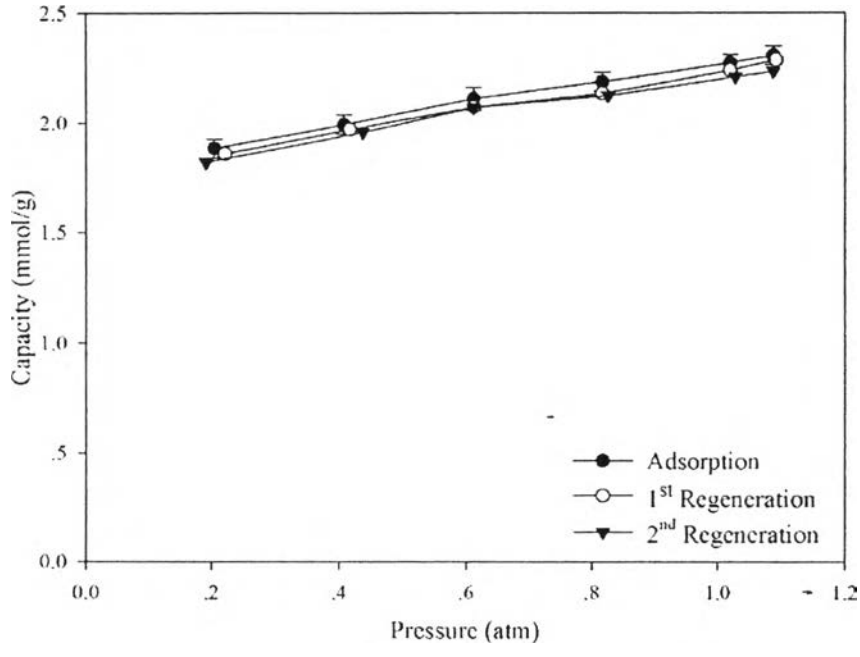

Figure 4.34 CO_2 adsorption isotherms at 50 °C of the 0.27 wt% PBZ/CSAC and the regenerated adsorbent.

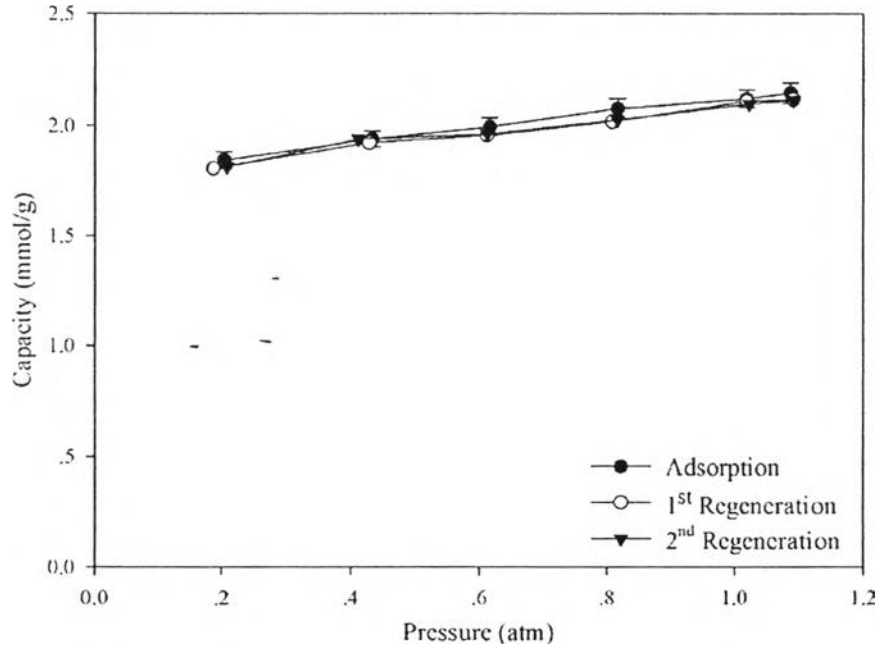

Figure 4.35 CO_2 adsorption isotherms at 50 °C of the 0.92 wt% PBZ/CSAC and the regenerated adsorbent.

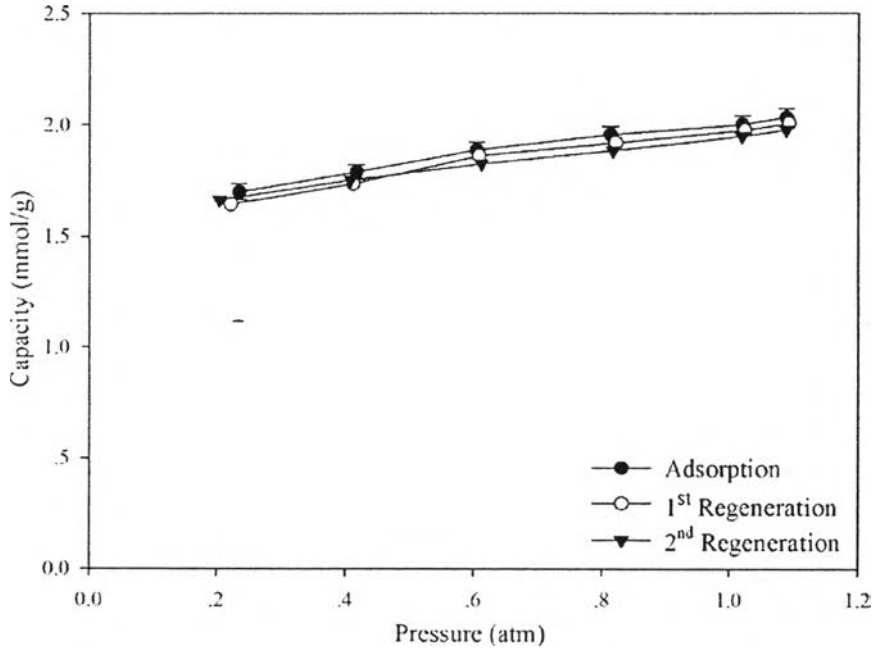

Figure 4.36 CO_2 adsorption isotherms at 50 °C of the 2.60 wt% PBZ/CSAC and the regenerated adsorbent.

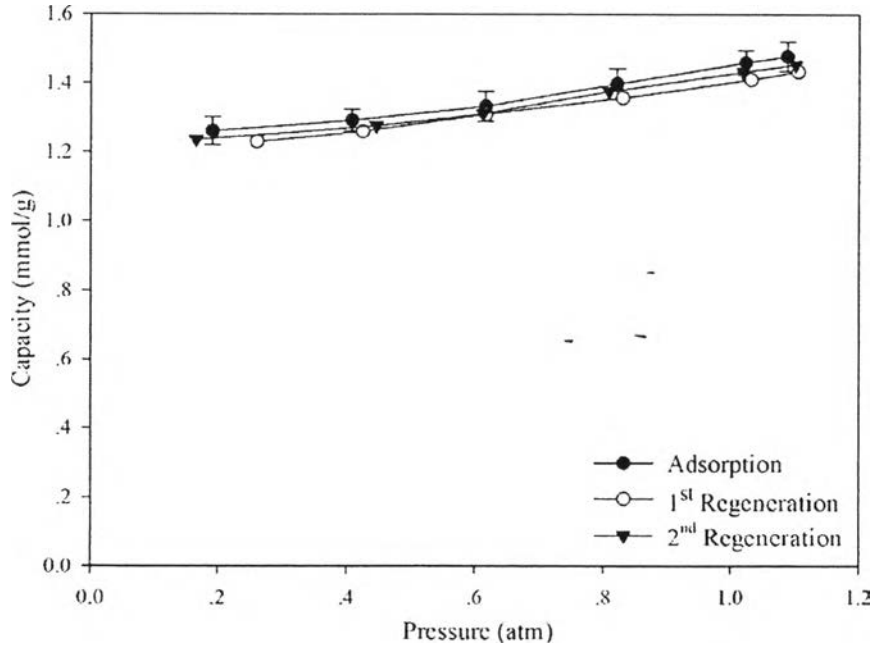

Figure 4.37 CO_2 adsorption isotherms at 75 °C of the 0.27 wt% PBZ/CSAC and the regenerated adsorbent.

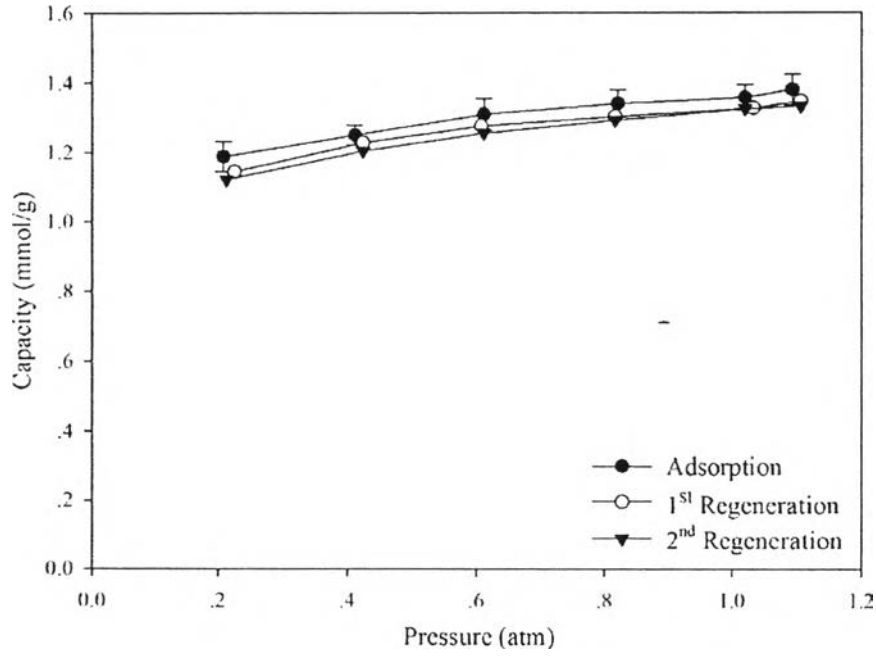

Figure 4.38 CO_2 adsorption isotherms at 75 °C of the 0.92 wt% PBZ/CSAC and the regenerated adsorbent.

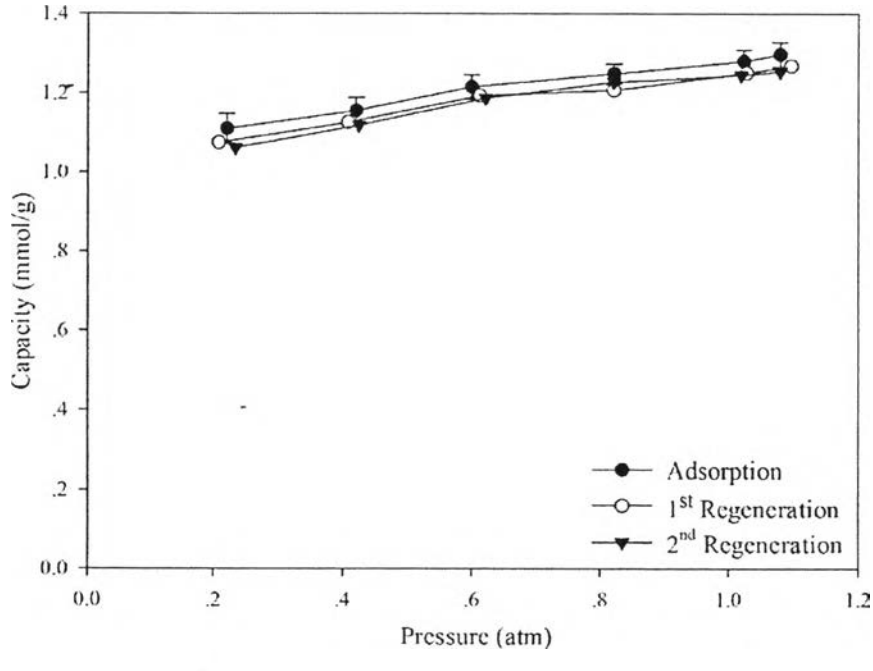

Figure 4.39 CO_2 adsorption isotherms at 75 °C of the 2.60 wt% PBZ/CSAC and the regenerated adsorbent.